Development of an In-Situ Hydrothermal Dissolved Carbon Dioxide Sensor for Hydrothermal Environments

Brooke Love

University of Washington, Seattle WA
Chemical Oceanography

Hydrothermal systems at mid ocean ridges are a unique environment which connect the mantle, lithosphere, ocean, and biosphere in one complex system. Fluid chemistry is one key tool in understanding this environment, and carbon dioxide is the most abundant gas in these fluids. Its relative abundance and the information it can give about the magmatic activity, which is one of the ultimate drivers of these systems, and other processes, make it an attractive target for development of an in-situ sensor. This work has shown that attenuated total reflection (ATR) is a promising technique for in situ carbon dioxide measurements under hydrothermal conditions. This redesign of the hydrothermal carbon dioxide instrument has yielded a sensor that functions well in laboratory tests and has been calibrated between 0 and 250 mmol/L CO_2. Mirrored surfaces and rounded faces on the ATR crystal were found to be problematic. An ATR element in the form of a truncated cone may be most appropriate in this aggressive environment and will be used in the next iteration. The high temperature, high pressure seal around the ATR element proved to be the most challenging part of the design, however a graphite seal was tested successfully and will be used in the next instrument. A coating of silicone was an effective method of water exclusion from the optical path length, even at high pressures. Finally, coupling of light into, and out of, the light pipes was far more critical than the output and sensitivity of the source and detector themselves. This work has brought us significantly closer to realizing real time, in situ measurements of sea floor hydrothermal carbon dioxide flux.

INTRODUCTION

Hydrothermal systems at mid-ocean ridges are unique and complex environments at the intersection of ocean, lithosphere, mantle and biosphere processes. Many of the interactions between these realms can be investigated through hydrothermal fluid chemistry. *In situ* instrumentation is of growing importance as hydrothermal studies and oceanography as a whole make a transition from expeditionary science to observatory based science. A key step forward will be the installation of a Regional Cabled Observatory (RCO) on the Juan de Fuca Plate in 2007-2008 by NEPTUNE Canada (www.neptunecanada.ca) followed by the U.S. NEPTUNE implementation. As this major infrastructure link becomes available, a wide variety of instrumentation must be developed in parallel in order to make the most effective use of this new and powerful resource.

Carbon dioxide is usually the most abundant hydrothermal gas, and it can vary dramatically in hydrothermal systems on both spatial and temporal scales [1-4]. This variation is related to phase separation, and more importantly, to magmatic activity, which is one of the ultimate drivers of these systems. Earthquakes and magmatic events can cause major episodes of fluid flux from the crust into the deep ocean, bearing nutrients and microbial biomass in large quantities [5-10]. The commonly used technique for characterization of volatiles in hydrothermal fluid, i.e. the collection of discreet samples in gas tight bottles, which are then analyzed in a shore-based laboratory, cannot capture the spatial and temporal characteristics of these systems. In order to capture the real variability and to quantify fluxes, it is necessary to employ a suite of *in situ* sensors that are capable of long-term deployments, and ideally of real time interactive measurement. Here we present the development of an in situ carbon dioxide (CO_2) sensor for use in high temperature hydrothermal vents.

ATTENUATED TOTAL REFLECTION

The CO_2 instrument is based on the attenuated total reflection (ATR) technique. This measurement is similar to infrared transmission spectroscopy, where the attenuation in the signal at a given wavelength is relative to the concentration of the absorbing species in the fluid. In water, which is highly absorbing in the infrared, the path length must be less than about 30 microns. This optimizes path length while preventing complete absorption by water at the CO_2 wavelength [11]. ATR allows for this very short interaction of the light with the fluid by controlling the number of reflections in a measuring crystal. Each time the light experiences a total internal reflection, it penetrates a small distance into the surrounding fluid, interacting with any absorbing molecules in the fluid before continuing on its reflected path (Figure 1). Each reflection produces a depth of penetration into the fluid that is on the order of one wavelength. (Equation 1) Actual path length depends on the polarization of the light, but is proportional to the depth of penetration. [12-15]

Equation 1:

$$\delta \approx \frac{\lambda}{2\pi n_1 \sqrt{\sin^2\theta - n_{21}^{\ 2}}}$$

Where δ is depth of penetration, λ is wavelength, n_1 is index of refraction of the crystal, θ is the angle of incidence and n_{21} is the ratio of the index of refraction of the fluid to the crystal.

The ATR technique is widely used in research and industry where transmission measurements are not practical because of highly absorbing species, or where surface associated processes are of interest. It has recently been used to investigate phenomena including polymerization of thin films, bacteria detection in food, quality control of pharmaceutical production, biofilm formation and many other areas of enquiry in chemistry, medicine and natural science [16-21]. Although many ATR accessories exist for infrared spectroscopy, none are configured to withstand the extreme conditions of temperature and pressure in hydrothermal systems.

INSTRUMENT DESIGN

A prototype ATR instrument was developed in 2005. A general schematic configured for a field deployment is illustrated in Figure 2. It includes light source, light pipes, ATR element, and detectors as well as the pressure housings and support electronics. Light is generated at an infrared source containing a diamond like thin film which reach temperatures up to 1000°C in a fraction of a second (85% modulation at 5 Hz). The light is directed to the crystal using a gold mirrored light pipe. Light pipes are necessary in order to distance the electronic components from the high temperature at the measurement point, which can exceed 400°C. Traditional fiber optics cannot be used because these fibers have a wavelength cutoff that is too low, and specialty infrared fibers cannot withstand the elevated temperatures [22]. The light pipes, fabricated by Epner Technologies, are coated with a highly reflective and scratch resistant gold, called Laser Gold. This material is the National Institute of Standards and Technology standard (#2011) for infrared reflective material and performs very well under extreme conditions. In fact, it is the coating used on the large mirror of the Mars Orbital Laser Altimeter and other NASA instruments [23].

When the beam leaves the light pipe, the light undergoes three reflections in the sapphire ATR element. Each reflection allows the light to interact with the hydrothermal fluid that bathes the crystal. All parts in contact with the fluid are either sapphire or titanium for maximum environmental resistance. The light exiting the crystal is then collected by the second light pipe, which then directs the infrared radiation back to the pressure case and towards the detectors. Alignment between the pipes and the source and detectors is achieved using four miniature optical positioning stages (Edmund Optics 38-527)

The two side by side pyroelectric detectors are covered by narrow band pass filters, centered on the major CO_2 absorption peak and a reference wavelength (4.26 and 3.9 microns respectively)(Infratec LMM-262). The light intensity at the reference detector is determined by absorption by water, intrinsic losses in the optical system, the intensity of the source and any fouling that may have occurred on the crystal surface. The intensity on the CO_2 channel is determined by all the factors above, plus absorption by CO_2 molecules in the fluid path length. Therefore the ratio of the two signals is a measure of CO_2 concentration that is largely independent of source strength, fouling and other factors. The reference wavelength is chosen to be as close as possible to the measurement wavelength so that they will be affected equally by physical changes in the system. The two detectors are also encapsulated in the same TO5 housing in order to minimize environmental differences between the two channels.

The voltage information for each channel is sent to a data logger (Onset Tattletale 8) in a separate pressure case, which also houses the batteries. The fluid temperature is measured

using a titanium clad type K thermocouple that has been extensively tested and successfully deployed many times in the past. The ambient temperature in the case can affect the voltage output of the detector; therefore a reading is taken from a thermistor mounted directly on the amplifier board next to the detector. The case temperature is expected to remain nearly constant *in situ* because of the heat sink capacity of the surrounding seawater.

The optical crystal is a sapphire prism. Sapphire is the material of choice for demanding optical applications. It is extremely chemically resistant, optically clear up to a wavelength of five microns, and is surpassed in hardness only by diamond [22]. Cubic zirconia was also considered as a crystal material. Its optical and chemical properties are ideal, but a large thermal expansion coefficient makes it prone to shatter. Lab tests showed that upon a sudden change of temperature, such as going from hot hydrothermal fluid into cold seawater, there was an unacceptable level of breakage of zirconia crystals. Castable ceramic insulation that would dissolve slowly in the hydrothermal fluid did not decrease the breakage to a sufficient degree to allow us to proceed with zirconia crystals.

The system is designed with two pressure cases in order to make the wand assembly light and maneuverable and to keep the stored data safe. Only the most critical optical components are housed in the small pressure case, so that if a leak were to occur in the high temperature part of the instrument, only a few parts would be lost, and all data recorded to that point would be preserved.

CALIBRATION AND PRELIMINARY RESULTS

A method was developed for generating specific concentrations of dissolved carbon dioxide, and using them to calibrate the sensor. Solutions of known concentrations of sodium carbonate and hydrochloric acid are kept in large reservoirs. One high pressure pump draws from each reservoir, at pump rates that combine the two components such that the carbonate will be present almost completely as carbon dioxide, at a pH of about 3. The two streams are combined on the high pressure side of the system to prevent the CO_2 from escaping solutions that would be supersaturated at ambient pressure. The calibration solution then passes through the measurement cell and the back pressure regulator.

Immediately after leaving the regulator, the fluid passes through a valve which can direct the flow into a large syringe. The actual CO_2 concentration can be determined manometrically by comparing the volume of gas and mass of water collected after they have reached equilibrium at ambient conditions. At low CO_2 levels, the pump rates and fluid concentrations are used to calculate concentration.

When the flow is not directed into the syringe port for collection, it flows past a pH electrode. The real time reading of pH allows small adjustments to be made to the flow rates in order to maintain optimum pH levels. pH is monitored in the lab to ensure complete conversion of carbonate and bicarbonate to carbon dioxide by the addition of the appropriate amount of hydrochloric acid. In the field, this will not be necessary as the in-situ pH is stable and ensures that the carbonate in the fluids is present as CO_2.

A calibration was carried out on the prototype instrument at CO_2 levels up to 400 mmol/kg and at pressures between 60 and 100 bar (Figure 4). Pressure was limited by the seals on the

first version of the calibration pressure cell. The sensor predicted actual concentration with a correlation coefficient as high as 0.997 and with standard errors as low as 6 mmol/kg. Further testing of this prototype was made impossible when repeated breaking and recompression of the high pressure seals caused a crack in the ATR crystal.

SECOND GENERATION SENSOR

Many changes were made to the design of the instrument between the first and second generation. Most were aimed at increasing the reliability and strength of the sensor, as well as improvements in sensitivity.

Infrared Detector:

The prototype instrument used an LIM-262 pyroelectric dual channel detector from Infratec. This pyroelectric detector responds to changes in incoming radiation, rather than to the overall amount of radiation which means more complicated signal processing. It was replaced by a thin-film bismuth antimony thermopile detector (Dexter Research DR46). The detectivity (an overall figure of merit) is increased from 2.4×10^8 to 3.2×10^8 cm$\sqrt{\text{Hz}}$/W. The new detector is also not sensitive to microphonic noise, which was a problem in the pyroelectric detector.

The simplification in signal processing did prove to be helpful, but the time to reach a stable signal did not improve because the limiting factor is the source rather than the detector. Results from optical testing show that the spacing between detectors for the two channels is an important factor. Although the greatest voltage response for a single channel was seen on the LIM detector, when response was balanced between two channels with the light pipe in place, the Dexter performed better because the two detectors are more closely spaced.

Infrared Light Source:

Infrared sources usually consist of a thin film or filament that is heated resistively to emit broadband infrared light. Sources of this type were investigated, as well as a new class of narrowband LED emitters. The LEDs, though much improved in recent years, still could not provide enough optical power for this application. A resistive source with a parabolic reflector was used in the first sensor. The overall diameter of the reflector was greater than that of the light pipe, so the light pipe was inserted into the reflector up to the point where their diameters were similar. This led to the collection of a fairly large proportion of light that was not parallel or sub-parallel to the axis of the light pipe and was unlikely to propagate all the way to the detector (about 1/3 of coupled light was unusable). The new instrument was designed to use a source with an elliptical reflector (Calsensor SVF350-5M) where the filament is at one focal point and the opening of the light pipe is at the other (Figure 4). This should have resulted in a more parallel and collimated beam, and better optical throughput.

Testing of the actual source showed that the elliptical reflector did a poor job of focusing the light at the focal length, and therefore coupling of light into the light pipe was severely compromised. Overall, the arrangement that gave the best coupling was to use a thin film source (ICX Photonics NM5NSC) with no reflector, with some degree of light gathering and collimation achieved with a sapphire ball lens at the inlet to the light pipe.

Crystal Design:
The prototype instrument used a prism shaped measurement crystal. This design allowed simple prediction of pathlengths because all rays would follow approximately the same path, and make their reflections at the same angles. However two significant problems were encountered. First, this design necessitated mirrored surfaces on the crystal. This was achieved by vapor deposition of gold on these surfaces. This gold layer proved to be exceedingly delicate. Efforts to mitigate this problem were only partially successful. Secondly, the performance of such a design is limited in the temperature conditions under which it will work, because the angle of incidence of the light is always the same while the index of refraction of the fluid and the critical angle, are changing with temperature. (See equation 1.)

A hemispheric crystal circumvents the problems mentioned above. The incoming light is directed to a portion of the surface of the hemisphere where the angle of incidence is sufficiently high to cause a total reflection without the need for any mirrored surfaces, and the angle of incidence varies across the illuminated spot on the surface, making for a more flexible and robust design. Optical modeling predicted an acceptable optical throughput for this design, but when tested, light loss in the system was extreme. This may be due to a large proportion of light incident upon the surface at very close to the critical angle. These rays are difficult to model because of non-linear behavior close to the critical angle, and actual absorption losses to water exceeded those of the model.

A thin layer of silicone polymer was applied to the measuring surface of the sapphire to minimize attenuation by water. The silicone allows the dissolved gasses to diffuse into the measurement space, but excludes most of the water which absorbs so much of the infrared radiation from the thin layer above the surface of the sapphire. This proved an effective technique to boost optical throughput, though it limits the temperature range in which the instrument can be deployed. Future versions will revert to a prismatic design that does not require mirrors. A truncated cone may be a good compromise, combining the ease of sealing to a cylindrical cross section, and the predictable path length allowed by the simple geometry.

High Pressure Seal:
One of the most problematic tasks in designing an instrument for hydrothermal systems is maintaining a high pressure, high temperature seal. The original seal around the prismatic crystal was accomplished using gold gaskets and high compressive forces. These seals were inflexible and fragile. They were replaced with Kalrez o-rings, which allowed us to complete our initial testing, but these are not resistant enough to withstand long deployments at high temperature conditions. A titanium to sapphire braze seal was made on an in situ ramen instrument developed in cooperation with our lab. [24, 25]. That seal, between a sapphire ball and the tip of a titanium probe, made by PA&E, Electronics for Extreme Environments, performed extremely well under both lab-testing conditions and in deployment in high temperature vents. This technique was also used to seal the sapphire hemisphere to the tip of the titanium wand holding the light pipes in this instrument.

The first attempt to make this seal failed when the sapphire broke several days after the seal was made. The second sapphire was modified to give it beveled edges which were expected

to minimize accumulation of stress at the weak corners of the crystal, and an inert, rather than an active braze material was used. These modifications were not effective, and the sapphire also broke on the second attempt (Figure 5). The basic problem seems to be a slight mismatch in the thermal expansion coefficients of sapphire and titanium. This is compounded by the fact that the hemispheres were made with the flame fusion method, which produces crystals that are prone to cracking. The third hemisphere was secured into the tip using a high strength epoxy to allow some lab testing to be carried out without breaking the last remaining crystal.

Although it cannot be used with the hemispherical crystal, we have tested a seal that will work for the next sensor design. A graphoil seal from Conax Buffalo has been tested on a ½" sapphire rod, and has held to a full pressure of 4500 psi. This seal involves the compression of a graphite ferrule onto an extended cylindrical section at the back of the ATR element. Although it will mean greater absorptive losses in the sapphire, this seal is chemically resistant and it will hold to full temperature and pressure.

Asymmetric Light Pipes:
The first sensor used two light pipes of the same size for sending and collecting the infrared light. The size of the collection pipe is determined mainly by the size of the detector. The other light pipe was made the same size for simplicity of design and procurement. However, with the addition of the hemispheric crystal, the location of the incoming beam on the surface of the crystal becomes more important. There is only a limited area where the angle of incidence will allow a reflection to occur and where that reflection will result in sufficient path length in the fluid for a measurement to be made. Therefore, a smaller diameter light pipe (3mm diameter) was used to direct the light to the optimal area of the measurement crystal surface while the larger diameter light pipe collected as much of that light as possible and sent it to the detectors. Future designs will not require the smaller spot size and the larger 4 and 6 mm diameter light pipes, which are much easier to couple to, will be used.

The modifications to the sensor design outlined above are the results of extensive modeling of the system using Zemax-EE Optical Design Program (Figure 6). Size and shape of the optical crystal as well as size, location and orientation of the light pipes were tested in numerous configurations to determine which would yield the best optical throughput and path length through the largest range of conditions. Ten thousand rays were used in the analysis of each scenario. These ray traces were then exported to Matlab where the strength of the ATR interaction was calculated.

RESULTS

The calibration method developed for the prototype instrument was used in the testing of the second generation instrument as well. The pressure cell has a compact design with minimal dead volume (Figure 7). An initial calibration was carried out between 0 and 275 mmol/L of carbon dioxide at room temperature and 60 bar. (Figure 8) These conditions were chosen for the initial test in order to make the calibration easily comparable to the first generation results. This first calibration yields an R^2 of 0.96 and a standard error of 8 mmol/L when only the ratio

and CO_2 concentration are considered. The inclusion of temperature and pH in the calibration would no doubt improve the fit for future calibrations.

The effects of added temperature and pressure are expected to be small. This calibration was carried out at room temperature, but the molecular absorbtivity of carbon dioxide increases significantly with temperature. Between 0 and 300 C it increases by over 75%, leading to a proportional increase in sensitivity [26]. The DR46 detector currently in use is also equipped with a filter that is better suited to the center wavelength and width of the absorption peak at high pressure, eliminating much of the adverse effect of pressure seen in figure 3. Therefore we can expect more sensitivity to carbon dioxide and less noise at *in situ* conditions with the redesigned sensor

CONCLUSIONS

This work has shown that attenuated total reflection is a promising technique for in situ carbon dioxide measurements in hydrothermal conditions. The sensor functions well in laboratory tests and has been calibrated to a wide range of CO_2 concentrations, spanning those measured in hydrothermal systems. We have shown that an ATR element using beveled faces rather than a rounded lens is most appropriate, and that mirrored faces are too delicate for this aggressive environment. The high temperature, high pressure seal proved to be the most challenging part of the design, however a graphite seal was tested successfully and will be used in the next instrument. A coating of silicone was an effective method of water exclusion, even at high pressures, and coupling of light into and out of the light pipes was far more critical than the output and sensitivity of the source and detector themselves. The light pipes, source, detectors, temperature monitoring system, data logger, and pressure cases can be used in the next sensor design without modification. This work has brought us significantly closer to realizing real time, in situ measurements of sea floor hydrothermal carbon dioxide output.

ACKNOWLEDGEMENTS

I would like to acknowledge some of the many people who have been instrumental in the completion of this research. Marilyn C. Link and the Link Foundation have generously supported this work, along with funding from the Keck Foundation. Marv Lilley has been immensely helpful and patient throughout this project. Many people in industry have been extremely generous with their time and advice, including David Cutter at PA&E, Mike Pollack at EnvirOptics, Anthony DeFeo at Guild Optics, , Paul Wilks of Wilks Enterprise Inc., David Epner of Epner Technologies, and Steve Hudlet of Jet Seal. Eric Olson, David Demaray, Mike Vinton, Steve Elliot and Rex Johnson at the University of Washington have been invaluable parts of the team that has made this work possible.

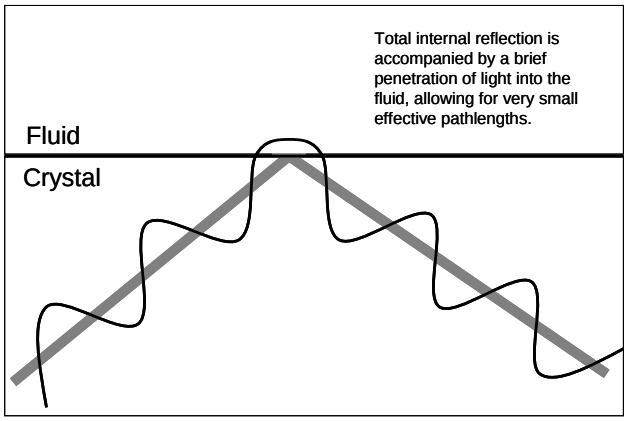

Figure 1

Attenuated Total Reflection: The path length that the light travels through the fluid is determined by indexes of refraction, wavelength and angle of incidence. The field strength decays exponentially away from the surface and effective penetration depth is on the order of one wavelength.

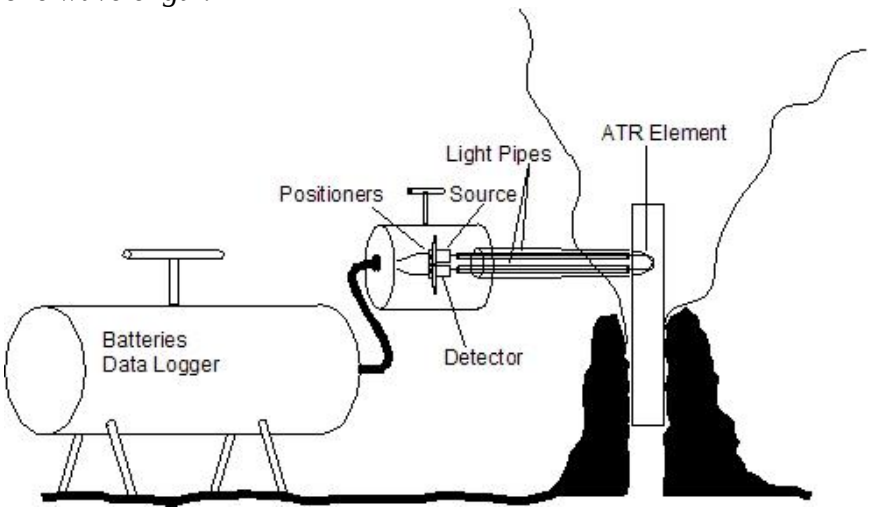

Figure 2

Schematic of deployment in a high temperature vent, including large and small pressure cases, and sampling wand.

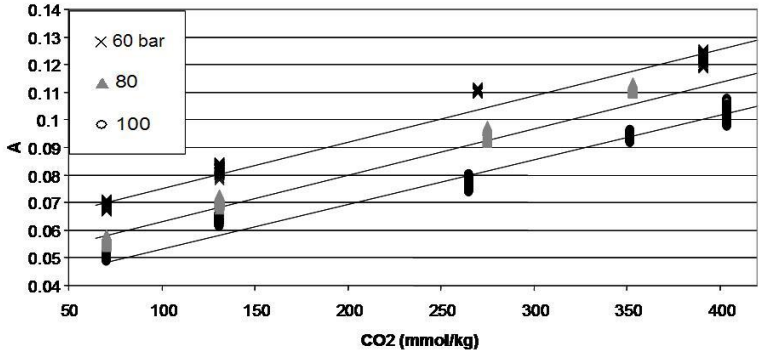

Figure 3

Preliminary test results show consistent response of the sensor (Absorbance) to CO_2 concentration at three pressure levels. Correlation is better than appears in this plot as the variance due to case temperature (not represented here) is included in the regression.

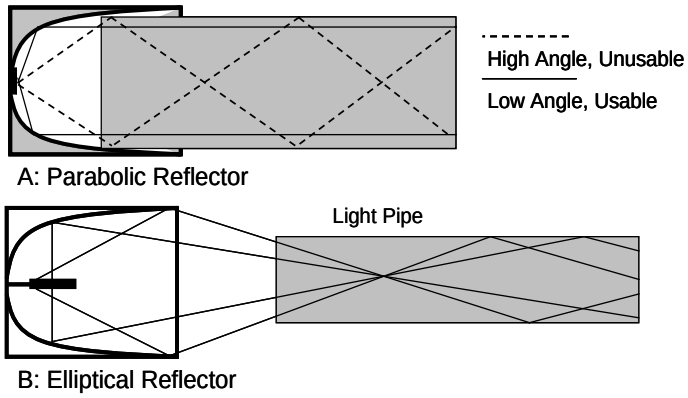

Figure 4
The orientation of the infrared element and the elliptical shape of the reflector should combine to give design B a greater proportion of usable light propagating through the system. This does not prove to be the case because of poor focusing capability.

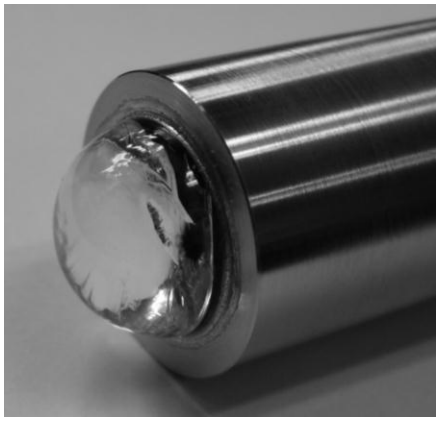

Figure 5
The cracked hemisphere after an attempted braze.

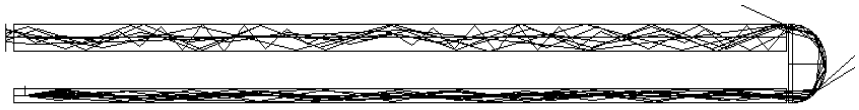

Figure 6
Results of an optical model showing 25 rays propagating through the system; 10,000 rays were used for analysis of each configuration

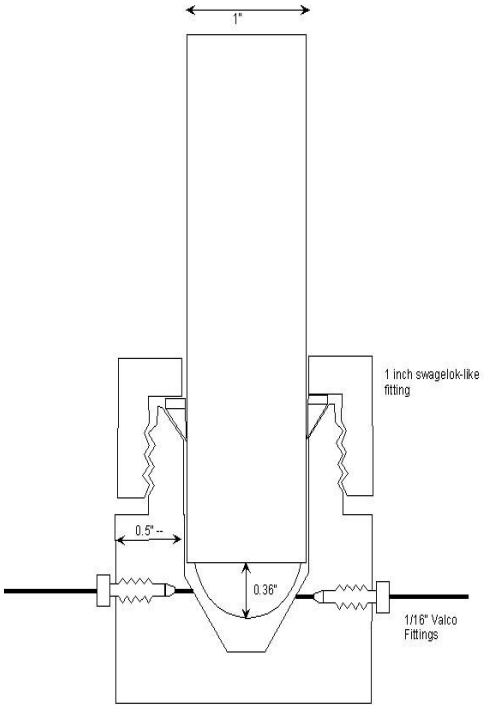

Figure 7

Laboratory pressure cell of compact design: low dead volume allows ease of switching solutions, low thermal mass makes heating simple, Swagelok type seals and titanium construction give high maximum temp and pressure limits.

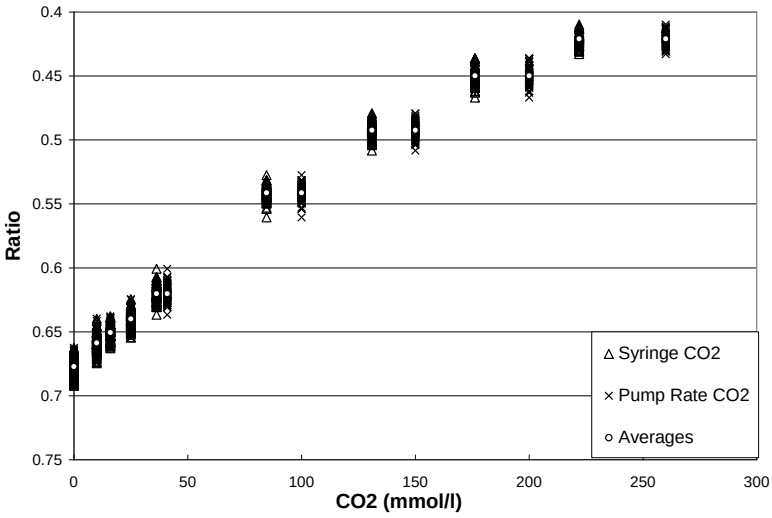

Figure 8
Initial calibration results from the second-generation instrument. Two different methods of calculating the CO2 are included here. A departure from linear response is evident at high concentrations.

References

1. K.L. VonDamm, L.G. Buttermore, S.E. Oosting, A.M. Bray, et al., "Direct observation of the evolution of a seafloor 'black smoker' from vapor to brine" *Earth and Planetary Science Letters*, **149**(1-4): 101-111 (1997)
2. D.A. Butterfield, I.R. Jonasson, G.J. Massoth, R.A. Feely, et al., "Seafloor eruptions and evolution of hydrothermal fluid chemistry" *Philosophical Transactions of the Royal Society of London Series a-Mathematical Physical and Engineering Sciences*, **355**(1723): 369-386 (1997)
3. D.A. Butterfield, R.E. McDuff, M.J. Mottl, M.D. Lilley, et al., "Gradients in the Composition of Hydrothermal Fluids from the Endeavor Segment Vent Field - Phase-Separation and Brine Loss" *Journal of Geophysical Research-Solid Earth*, **99**(B5): 9561-9583 (1994)
4. M.D. Lilley, D.A. Butterfield, J.E. Lupton, and E.J. Olson, "Magmatic events can produce rapid changes in hydrothermal vent chemistry" *Nature*, **422**(6934): 878-881 (2003)
5. J.R. Delaney, D.S. Kelley, M.D. Lilley, D.A. Butterfield, et al., "The quantum event of oceanic crustal accretion: Impacts of diking at mid-ocean ridges" *Science*, **281**(5374): 222-230 (1998)
6. J.A. Huber, D.A. Butterfield, and J.A. Baross, "Bacterial diversity in a subseafloor habitat following a deep-sea volcanic eruption" *Fems Microbiology Ecology*, **43**(3): 393-409 (2003)
7. J.A. Huber, H.P. Johnson, D.A. Butterfield, and J.A. Baross, "Microbial life in ridge flank crustal fluids" *Environmental Microbiology*, **8**(1): 88-99 (2006)
8. D.S. Kelley, J.A. Baross, and J.R. Delaney, "Volcanoes, fluids, and life at mid-ocean ridge spreading centers" *Annual Review of Earth and Planetary Sciences*, **30**: 385-491 (2002)
9. J.R. Marchesi, A.J. Weightman, B.A. Cragg, R.J. Parkes, et al., "Methanogen and bacterial diversity and distribution in deep gas hydrate sediments from the Cascadia Margin as revealed by 16S rRNA molecular analysis" *Fems Microbiology Ecology*, **34**(3): 221-228 (2001)
10. E. Davis, K. Becker, R. Dziak, J. Cassidy, et al., "Hydrological response to a seafloor spreading episode on the Juan de Fuca ridge" *Nature*, **430**(6997): 335-338 (2004)
11. M.L. Kieke, J.W. Schoppelrei, and T.B. Brill, "Spectroscopy of hydrothermal reactions .1. The CO2-H2O system and kinetics of urea decomposition in an FTIR spectroscopy flow reactor cell operable to 725 K and 335 bar" *Journal of Physical Chemistry*, **100**(18): 7455-7462 (1996)
12. F.d. Fornel, *Evanescent waves : from Newtonian optics to atomic optics*. 2001, Berlin ; New York: Springer. xvii, 268 p.
13. N.J. Harrick, "Electric Field Strengths at Totally Reflecting Interfaces" *Journal of the Optical Society of America*, **55**(7): 851-& (1965)
14. N.J. Harrick, M. Milosevic, and S.L. Berets, "New Developments in Internal-Reflection Spectroscopy .2. The Horizon" *American Laboratory*, **24**(9): 29-32 (1992)
15. M. Milosevic, "Internal reflection and ATR spectroscopy" *Applied Spectroscopy Reviews*, **39**(3): 365-384 (2004)

16. K.R. Park, P.H. Kang, and Y.C. Nho, "Preparation of PFA-g-polystyrene sulfonic acid membranes by the gamma-radiation grafting of styrene onto PFA films" *Reactive & Functional Polymers*, **65**(1-2): 47-56 (2005)
17. M.E. Goldberg and A.F. Chaffotte, "Undistorted structural analysis of soluble proteins by attenuated total reflectance infrared spectroscopy" *Protein Science*, **14**(11): 2781-2792 (2005)
18. R. Linker, I. Shmulevich, A. Kenny, and A. Shaviv, "Soil identification and chemometrics for direct determination of nitrate in soils using FTIR-ATR mid-infrared spectroscopy" *Chemosphere*, **61**(5): 652-658 (2005)
19. H. Yang, S.A. Ibrahim, and C.W. Seo, "Rapid detection, identification, and enumeration of bacteria in foods using FTIR-ATR spectroscopy with chemometrics" *Abstracts of Papers of the American Chemical Society*, **229**: U50-U50 (2005)
20. M.R. Sohrabi, M. Davallo, F. Tadayyon, F. Nabipoor, et al., "Simultaneous determination of acetyl salicylic acid and acetaminophen in acetaminophen-caffeine-aspirin (ACA) tablets by FT-IR/ATR spectrometry with multivariate calibration data treatment" *Asian Journal of Chemistry*, **17**(1): 541-547 (2005)
21. J. Schmitt, D. Nivens, D.C. White, and H.C. Flemming, "Changes of biofilm properties in response to sorbed substances - An FTIR-ATR study" *Water Science and Technology*, **32**(8): 149-155 (1995)
22. M. Saad, *Infrared glass optical fibers and their applications : 15-16 July, 1998, Quebec, Canada*, ed. M. Saad. 1998, Bellingham, Washington :: SPIE. ix, 254 p. :.
23. M.A. Kreslavsky and J.W. Head, "Kilometer-scale slopes on Mars and their correlation with geologic units: Initial results from Mars Orbiter Laser Altimeter (MOLA) data" *Journal of Geophysical Research-Planets*, **104**(E9): 21911-21924 (1999)
24. T.M. Battaglia, E.E. Dunn, M.D. Lilley, J. Holloway, et al., "Development of an in situ fiber optic Raman system to monitor hydrothermal vents" *Analyst*, **129**(7): 602-606 (2004)
25. B. Dable, B. Love, T. Battaglia, Booksh K, et al., ""Characterization and Quantitation of a Tertiary Mixture of Salts by Raman Spectroscopy in Simulated Hydrothermal Vent Fluid" " *Applied Spectroscopy Reviews*, (Submitted 9/05)
26. P.G. Maiella, J.W. Schoppelrei, and T.B. Brill, "Spectroscopy of hydrothermal reactions. Part XI: Infrared absorptivity of CO2 and N2O in water at elevated temperature and pressure" *Applied Spectroscopy*, **53**(3): 351-355 (1999)